Magnetic excitations and dynamical Jahn-Teller distortions in UO_2

R. Caciuffo
Istituto Nazionale per la Fisica della Materia, Dipartimento di Scienze dei Materiali e della Terra, Università di Ancona, Via Brecce Bianche, I-60131 Ancona, Italy

G. Amoretti
Istituto Nazionale per la Fisica della Materia, Dipartimento di Fisica, Università di Parma, Parco Area delle Scienze 7A, I-43100 Parma, Italy

P. Santini
Institut de Physique Théorique, Université de Lausanne, CH-1015 Lausanne, Switzerland

G. H. Lander
European Commission, Joint Research Center, Institute for Transuranium Elements, Postfach 2340, D-76125 Karlsruhe, Germany

J. Kulda
Institut Laue Langevin, Avenue des Martyrs, Boîte Postale 156 X, F-38042 Grenoble, France

P. de V. Du Plessis
Department of Physics, University of Witwatersrand, P.O. WITS 2050, Johannesburg, South Africa
(Received 17 December 1998)

Inelastic neutron scattering with polarization analysis has been used to study the evolution of the magnetic response across the antiferromagnetic to paramagnetic transition in a single crystal of uranium dioxide ($T_N = 30.8$ K). The spin-wave dispersion curves have been determined at 16 K by measuring the spin-flip channel of the neutron cross section along the principal crystallographic directions. Evidence of magnon-phonon interactions along the $(0,0,\xi)$ direction is given by the splitting of the lowest spin-wave branch, and by the Q dependence of the energy-integrated dynamic susceptibility. Above T_N, a magnetic inelastic response consisting of two dispersive peaks was observed between 3 and 10 meV. This signal was easily measurable even at 200 K, more than six times the Néel temperature, where spatial correlations between the uranium spins are essentially zero. We assume this result as evidence that in the time scale of our experiment the uranium triplet ground state is split into three singlets, due to a dynamical Jahn-Teller (JT) distortion of the oxygen cage which reduces the point symmetry at the uranium site. Since the position of the peaks and their dispersion are compatible to a 1-**k** distortion along the $\langle 100 \rangle$ direction, a picture emerges in which local, uncorrelated 1-**k** dynamical JT distortions occur above T_N along the three directions of the $\langle 100 \rangle$ star; as T_N is approached, a correlation builds up between the phases of the corresponding vibrations until, eventually, a static 3-**k** structure is obtained below T_N. [S0163-1829(99)09621-6]

I. INTRODUCTION

Uranium dioxide is a semiconductor, crystallizing in the fcc fluorite structure with lattice constant $a_0 = 5.470$ Å at room temperature. The U ions are tetravalent with the $5f^2$ levels lying in a 6-eV gap between the valence and conduction bands. Over thirty years ago, experiments with neutron diffraction[1] established the magnetic ordering wave vector and that the transition to the antiferromagnetic (AF) state is discontinuous at $T_N = 30.8$ K. The ordered moment is $1.74\mu_B$ per uranium ion at low temperature. Within a year or so of these first reports, elastic constant measurements[2] established that there was strong coupling between the electronic and phononic systems (the c_{44} elastic constant starts to soften near ~ 200 K, almost 6.5 T_N). Allen proposed[3] a mechanism involving the distortion of the oxygen cage surrounding each uranium to account for this coupling. At the same time, extensive neutron inelastic measurements were reported by Cowley and Dolling,[4] and were interpreted as showing evidence of magnon-phonon interaction. This interaction is at the basis of the theory developed by Sasaki and Obata,[5] who proposed that a dynamical Jahn-Teller (JT) distortion can account for the anomalous behavior of the static magnetic susceptibility of $Th_{1-x}U_xO_2$ solid solution, for small values of x. Subsequent neutron-diffraction experiments[6] revealed that there was indeed a distortion of the oxygen cage, but it was not the one proposed by Allen.[3] Furthermore, with the deeper understanding of the so-called 3-**k** structures in the actinides,[7] Burlet *et al.*[8] proposed that UO_2 has such a 3-**k** magnetic structure. The moment distribution in a magnetically ordered crystal can be Fourier expanded whatever the nature of the magnetic ordering. A 1-**k** structure is obtained if only one wave vector **k** enter in the Fourier summation; in this case, the ordering is usually collinear and wave vectors equivalent to **k** under the symmetry operations of the paramagnetic point group (the so-called

star of the wave vector **k**) define separate magnetic domains. An n-**k** structure may be simply described as one in which n members of the star of **k** enter in the Fourier sum. The result is a noncollinear order. The AF structure of UO_2 is of type I, with Fourier components $\mathbf{m}_k$ perpendicular to the propagation vector $\mathbf{k}=(0,0,1)$. The 3-**k** structure is determined by the sum of the Fourier components corresponding to the three wave vectors $(1,0,0)$, $(0,1,0)$, and $(0,0,1)$. As a result, the symmetry remains cubic and the magnetic moments point along the $(1,1,1)$ directions of the cubic unit cell. This explains the fact that the crystal symmetry of UO_2 does not lower below T_N, as it should occur if the structure was 1-**k** or 2-**k**.

Later neutron inelastic scattering experiments to look for the dynamical softening of the phonon associated with a distortion of the oxygen cage did not find any conclusive evidence for such an effect, but, surprisingly, did report that the spin-wave spectra were more complicated than found in earlier work.[9] An attempt by Giannozzi and Erdös[10] to describe the static and dynamic properties of UO_2 on the basis of an effective quadrupole-quadrupole interaction, assuming a 3-**k** ordered structure and a distortion of the same symmetry, was only partially successful. In particular Allen's 1-**k** distortion was found to be energetically favored with respect to the 3-**k** one. The above, far from satisfactory, situation with respect to understanding the phase transition from a microscopic perspective is to be contrasted with the advances in describing the ground- and excited-state wave functions as deduced from crystal-field spectroscopy. Since UO_2 is a semiconductor, crystal field (CF) theory should work well as there are no conduction-electron states. Especially in the actinides, conduction electrons usually cause severe broadening of the $5f$ levels, and in most metallic systems undermine the usefulness of the CF approach.[11] Rahman and Runciman[12] predicted a large CF splitting in UO_2 with the Γ_5 triplet as the ground state. Experiments at spallation neutron sources, first[13] at IPNS (Argonne National Laboratory, USA) and then with much better resolution[14] at the ISIS (Rutherford-Appleton Laboratory, UK) source proved that the ground-state multiplet $J=4$ is split by only 180 meV, as compared to 620 meV predicted by Rahman and Runciman.[12] The large energy range, up to about 700 meV, accessible in the ISIS experiment was crucial to address this point. The energy gap between the ground state Γ_5 triplet and the first excited state (a Γ_3 doublet) is 150 meV; a further excited state, the Γ_4 triplet, is at 167 meV. From these data, the cubic CF parameters and wave functions were extracted. Below T_N a well-resolved splitting of the various transitions allowed from the ground-state was observed, and interpreted as a consequence of the 3-**k** JT distortion of the oxygen sublattice, the molecular field playing only a minor role. A surprising result was the observation of a splitting even at $T=35$ K, well into the paramagnetic phase, suggesting that a dynamical JT effect must persist above T_N. The motivation for the present experiments arose from two separate directions. On the one hand, it is increasingly recognized that quadrupolar and magnon-phonon interactions are important in $5f$ electron systems, examples are UPd_3,[15] URu_2Si_2,[16] UFe_2,[17] so the understanding of these effects in semiconducting UO_2, in which at least the CF ground-state is well known and the $5f$ electrons are well localized, represents an important first step before tackling the more complex problem of the intermetallic compounds. On the other hand, from an experimental point of view, great advances have been made over the last ten years in the availability of polarization analysis (PA) with neutrons, chiefly due to better Heusler alloy crystals and the ability to construct focusing monochromators and analyzers. Using PA has the great advantage that it cleanly separates the magnetic from the vibronic signal.[18] Thus our aim was to perform the whole experiment with polarization analysis: first to study the magnon dispersion curves and see whether direct evidence for magnon-phonon coupling can be obtained, and then, second, to study the evolution of the magnetism across the Néel temperature to see whether a direct measurement of a splitting of the Γ_5 triplet ground state can be measured in the paramagnetic phase. Of considerable significance in planning this experiment was the fact that we had available a very large (99 g) single crystal of excellent quality.

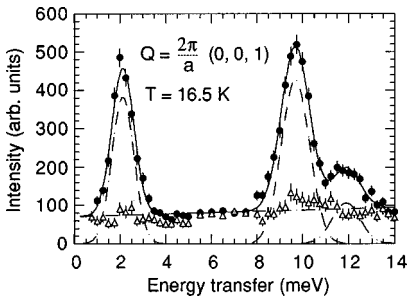

FIG. 1. Constant-**Q** scan at the $(0,0,1)$ antiferromagnetic zone center, at $T=16.5$ K. The data have been collected with an external magnetic field of 50 G parallel to the neutron-scattering vector **Q**. The spin-wave excitations appear in the spin-flip channel (closed circles); any signal of vibrational origin should appear in the non-spin-flip channel (triangles). The full line is a fit to the magnetic spectrum with a sloping background and three Gaussian line shapes (broken lines).

II. EXPERIMENTAL DETAILS

The single-crystal sample has been cut from a melt growth crystal boule of depleted uranium dioxide. It is a potato-shaped specimen of about 9 cm^3 in volume, with a homogeneous mosaic spread of about 0.4 degrees. Chemical and x-ray-diffraction analysis of small splinters confirm that the specimen is single phase and close to stoichiometry. The room temperature lattice constant $a=5.470(1)$ Å agrees well with values found in the literature.[1] The crystal was oriented with the $[1,-1,0]$ axis vertical, and placed in a Helium closed-cycle refrigerator. All measurements were made with the IN20 thermal neutron triple-axis spectrometer at the High Flux Reactor of the Institute Laue-Langevin, in Grenoble. A horizontally magnetized Cu_2MnAl Heusler curved (111) monochromator was used to polarize the incident beam and to select its energy. A similar Heusler crystal analyzer was employed to measure the energy and spin state of the scattered neutrons. A flat-coil dc flipper installed between the sample position and the analyzer provided the possibility to reverse the polarization of the incident beam. A flipping ratio $R=19\pm1$ was estimated from the peak inten-

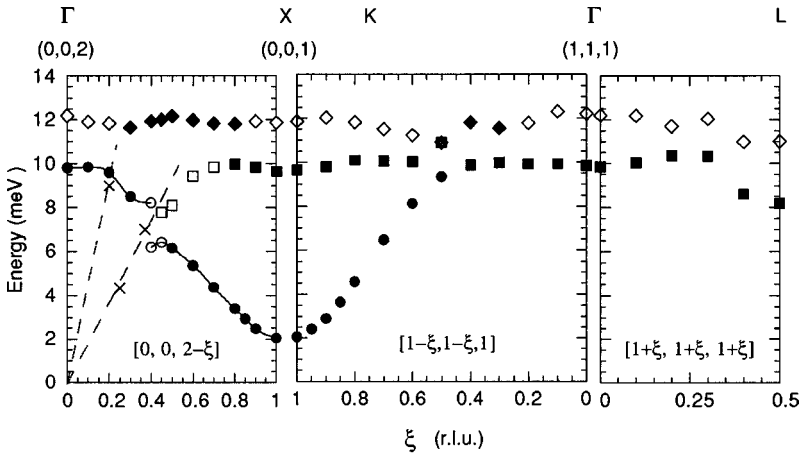

FIG. 2. Spin-waves dispersion curves measured at 16.5 K along the principal crystallographic directions. The broken lines and crosses correspond to acoustic phonon branches measured at 270 K. Magnon groups have been collected in the constant-**Q** mode, at the reciprocal lattice points $(0,0,2-\xi)$,$(1-\xi,1-\xi,1)$, and $(1+\xi,1+\xi,1+\xi)$. Open symbols indicate qualitatively smaller magnon intensity than the filled points. The non-spin-flip cross section was always found negligible. The solid line in the left panel is a guide to the eyes.

sity of the (002) Bragg reflection, measured with the flipper on and off. A magnetic field of 50 G was imposed at the sample position by a system of three Helmoltz coils, and oriented in such a way to maintain the incident neutron polarization along the direction of the momentum transfer **Q**. With the chosen geometry, the spin-flip (SF) and non-spin-flip (NSF) scattering intensities I_{SF} and I_{NSF} are given by

$$I_{SF}=\frac{1}{R-1}(RI_{ON}-I_{OFF})=I_M+\frac{2}{3}I_i^{sn}+B_{SF},$$

$$I_{NSF}=\frac{1}{R-1}(RI_{OFF}-I_{ON})=I_P+I_i^{isot}+\frac{1}{3}I_i^{sn}+B_{NSF}, \tag{1}$$

where I_{ON} and I_{OFF} are the intensities measured with the flipper on and off, respectively, I_M is the magnetic intensity, I_i^{sn} and I_i^{isot} are the nuclear-spin and isotopic-incoherent intensities, I_P is the phonon scattering, and B is the background. For the investigated sample, the incoherent scattering is very small and the spin-flip cross section is almost entirely of magnetic origin.

Data were taken at different temperatures T, from 16–300 K, using the constant-**Q** method and a fixed final energy of 14.68 meV. A pyrolytic graphite filter in the scattered beam was used to remove higher-order contamination. The horizontal collimation was 60′ before and after the sample, and 120′ between the analyzer and the detector. An energy scan about the (001) Bragg reflection has given a peak with a full width at half maximum (FWHM) of 0.5 meV; the FWHM of the Bragg peaks in typical Q scans was of about 0.02 Å^{-1}. The fall in intensity of the (100) magnetic Bragg peak across the Néel temperature locates the phase transition to the AF state in correspondence to a thermometer reading of 31.35 K.

III. RESULTS

A. $T<T_N$

The spin-wave dispersion curves have been determined at 16.5 K along the main crystallographic directions. Figure 1 shows a constant-**Q** scan at the (0,0,1) antiferromagnetic zone center. The uranium spin-wave excitations appear in the spin-flip channel (closed circles), while signals of vibrational origin should appear in the non-spin-flip channel (triangles). There are two intense peaks at about 2 and 10 meV and a smaller peak at about 12 meV, all showing magnetic character. The spin-waves dispersion curves are shown in Fig. 2, where the broken lines and crosses correspond to acoustic

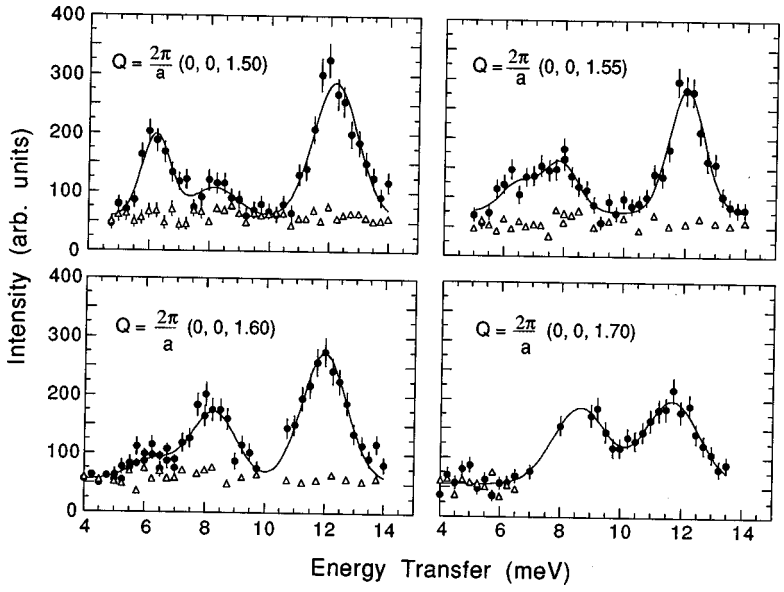

FIG. 3. Spin-flip (closed circles) and non-spin-flip (open triangles) neutron-scattering intensities at several $(0,0,2-\xi)$ points, for $0.3\leqslant\xi\leqslant0.5$ ($T=16.5$ K).

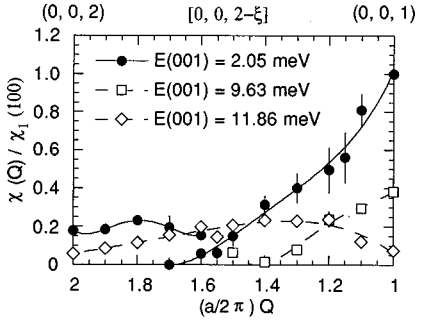

FIG. 4. Wave-vector dependence of the energy-integrated dynamic susceptibility of the three branches propagating along the $(0,0,\xi)$ direction, from $\mathbf{Q}=(2\pi/a)(0,0,2)$ to $\mathbf{Q}=(2\pi/a)(0,0,1)$. All data are normalized to $\chi_1(001)$, the value obtained at the magnetic zone center for the branch with lowest energy ($T=16.5$ K).

phonon branches measured at 270 K. The splitting of the lowest spin-wave branch due to the interaction with the TA phonon along $(0,0,\xi)$ is evident. All data have been collected in the constant-$\mathbf{Q}$ mode, at the reciprocal lattice points $(0,0,2-\xi)$, $(1-\xi,1-\xi,1)$, and $(1+\xi,1+\xi,1+\xi)$. Open symbols indicate qualitatively smaller magnon intensity than the filled points. The shape of these curves confirms the previous observations by Cowley and Dolling,[4] but the presence of extra branches, suggested by Buyers and co-workers,[9] is not confirmed. In particular, no evidence of splittings has been found at the X point $(0,0,1)$ for the two lowest magnetic modes, near 2.0 and 9.6 meV.

The points drawn in Fig. 2 have been deduced from the position of the peaks in the SF channel of the neutron cross section. Therefore all the observed branches present magnetic character over the whole Brillouin zone. This result differs from what is reported in Ref. 4, where a purely phonon character was attributed to the upper branch along the $(\xi,\xi,0)$, and (ξ,ξ,ξ) directions.

In Fig. 3 we show the SF and NSF neutron scattering intensities obtained at several $(0,0,2-\xi)$ points, for $0.3 \leqslant \xi \leqslant 0.5$. The intensity of the excitations belonging to the lowest $(0,0,\xi)$ branch becomes negligible around $\xi \approx 0.4$. Evidence of magnon-phonon interaction is given by the wave-vector dependence of the energy-integrated dynamic susceptibility, which is shown in Fig. 4 for the three branches propagating along the $(0,0,\xi)$ direction, from $\mathbf{Q}$

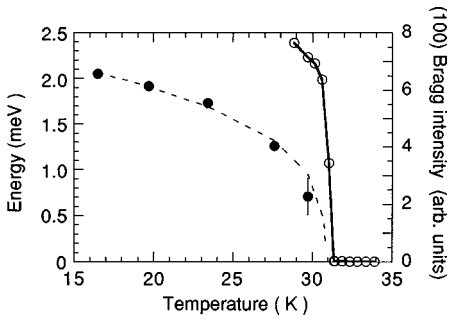

FIG. 5. Critical slowing down of the lowest energy spin-wave at $\mathbf{Q}=(2\pi/a)(0,0,1)$. The dashed curve is the hydrodynamic theory prediction, $E \propto (1-T/T_N)^{\nu/2}$, for a critical exponent $\nu=0.6$. The temperature dependence of the (001) Bragg-peak intensity (open circles) is also shown for comparison.

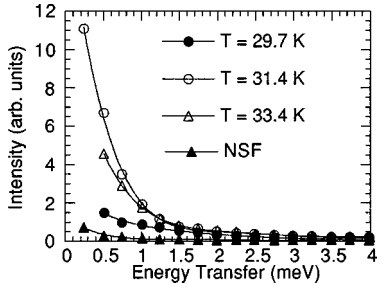

FIG. 6. Temperature dependence of the magnetic response at the X point $(0,0,1)$. The abrupt increase of intensity on warming through T_N is associated to the onset of dynamic critical scattering. The flat NSF signal gives an estimate of the background.

$=(2\pi/a)(0,0,2)$ to $\mathbf{Q}=(2\pi/a)(0,0,1)$. All data are normalized to $\chi_1(001)$, the value obtained at the magnetic zone center for the branch with lowest energy. The vanishing of the susceptibility for the two excitations indicated with dots and squares in Fig. 4 is related to the anticrossing with the transverse phonon branches (see Fig. 2). Without the magnon-phonon interaction, the magnon dispersion relations would be very different. In particular, the lowest branch would grow up to about 10 meV, with unchanged slope.

B. $T > T_N$

By increasing the temperature towards T_N, the critical slowing down of the lowest energy spin-wave at $\mathbf{Q}=(2\pi/a)(0,0,1)$ is observed. This is shown in Fig. 5, where the dashed curve is the hydrodynamic theory prediction, $E \propto (1-T/T_N)^{\nu/2}$, for a critical exponent $\nu=0.6$, and the open circles represent the temperature dependence of the (001) Bragg-peak intensity.

A large, Lorentzian-shaped, quasielastic response appears just above T_N around the antiferromagnetic zone center, the X point $(0,0,1)$. This signal is strongly temperature and Q dependent. Figure 6 shows the temperature variation of the magnetic response at $(0,0,1)$. The abrupt increase of intensity on warming through T_N is associated to the onset of dynamic critical scattering. Figure 7 shows the low-energy magnetic excitation spectra at $\mathbf{Q}=(2\pi/a)(0,0,1.05)$, above T_N. This point is chosen to avoid Bragg scattering near T_N and $\lambda/2$ contamination from the strong nuclear (002) reflection. The temperature dependence of the low-energy magnetic scattering FWHM at $\mathbf{Q}=(2\pi/a)(0,0,1.05)$ is shown in Fig. 8. Experimental data points have been obtained from a

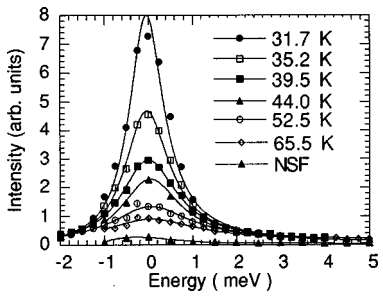

FIG. 7. Low-energy magnetic excitation spectra of UO_2 above T_N at $\mathbf{Q}=(2\pi/a)(0,0,1.05)$. The solid lines are fits to a flat background and a Lorentzian function multiplied by the Bose factor.

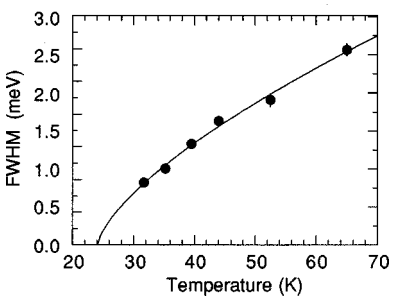

FIG. 8. Temperature dependence of the full width at half maximum of the low-energy magnetic scattering at $\mathbf{Q}=(2\pi/a)(0,0,1.05)$. Experimental data points have been obtained from a fit of the magnetic response to a Lorentzian line shape multiplied by the Bose factor and convoluted with the instrumental resolution. The solid line is a fit to a power law as indicated in the text.

fit of the magnetic response to a Lorentzian line shape multiplied by the Bose factor and convoluted with the instrumental resolution (solid lines in Fig. 7). The solid line in Fig. 8 is the fit to a power law of the form

$$\mathrm{FWHM}\propto(T/T^*-1)^{1.5\nu} \tag{2}$$

with $T^*=24\pm3$ K and a critical exponent $\nu=0.5\pm0.1$, close to the prediction of the Ginzburg-Landau model. The system would therefore exhibit a second-order phase transition at T^*, but the occurrence of the first-order phase transition at T_N prevents the susceptibility from diverging. Note that a similar value, $T^*=25\pm1$ K, was obtained from the behavior of the spatial magnetic correlation range, determined by critical diffraction experiments above T_N.[9]

Figure 9 shows the magnetic response at $T=31.7$ K and $\mathbf{Q}=\mathbf{G}+\mathbf{q}$, where $\mathbf{G}=(2\pi/a)(0,0,1)$ and $\mathbf{q}=(2\pi/a)(0,0,\xi)$. Solid lines are fit to Lorentzian line shapes multiplied by the Bose factor. The q dependence of the magnetic susceptibility along the $(0,0,\xi)$ direction at $T=31.7$ K is shown in Fig. 10. Experimental points are given by the energy integral of the dynamic susceptibility. As a visual aid, the data have been reflected in the zero-q axis. The fit to a Lorentzian function yields a spatial correlation length of 5.5(1) Å, almost the same value is reported by Buyers and Holden.[9] Figure 11 shows the FWHM of the low-energy magnetic response, at $T=31.7$ K, as a function of $q=(2\pi/a)\xi$. The solid line is a fit to the function $\Gamma=\Gamma_0+\alpha q^\gamma$, for $\Gamma_0=0.72$ meV, a spin-diffusion coefficient $\alpha=11$ and an exponent $\gamma=1.3$. A similar behavior was found for MnF_2, where the low-q experimental data are fitted by a power law with $\gamma=1.6$.[19]

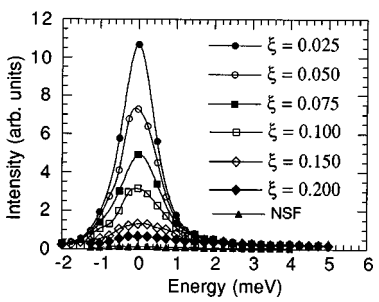

FIG. 9. Magnetic response at $T=31.7$ K and $\mathbf{Q}=(2\pi/a)(0,0,1+\xi)$. Solid lines are fits to Lorentzian line shapes multiplied by the Bose factor.

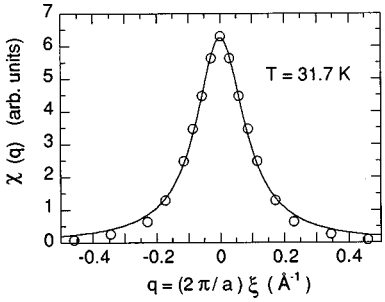

FIG. 10. Wave-vector dependence of the magnetic susceptibility along the $(0,0,\xi)$ direction at $T=31.7$ K. Experimental points are given by the energy integral of the dynamic susceptibility. As a visual aid, the data have been reflected in the zero-q axis. The solid line is the fit to a Lorentzian function.

A magnetic inelastic response is observed in the energy region between 3 and 10 meV, at least up to 200 K, which is about 6.5 times the Néel temperature. Figure 12 shows the magnetic excitation spectra at $T=65.5$ K and different $\mathbf{Q}=(2\pi/a)(0,0,\xi)$. Solid lines are the fit to a flat background and the superposition of two Lorentzian line shapes, which appear to be dispersive. The origin of these magnetic excitons will be discussed below.

IV. DISCUSSION

A. $T<T_N$

Our results for the magnon dispersion curves at 16.5 K (Figs. 1 and 2) confirm those of Cowley and Dolling.[4] We have no evidence of the extra points reported in Ref. 9, in particular around $\xi=0.7$ and for $0.15<\xi<0.4$ in the energy range 9–12 meV (in the notation of Fig. 2). For example, following Ref. 9, at $\mathbf{Q}=(2\pi/a)(0,0,1.60)$ an extra peak should be observed at about 9 meV, which would raise to about 10 meV at $\mathbf{Q}=(2\pi/a)(0,0,1.70)$. Our measurements seem to exclude the presence of this peak.

The additional modes were assumed in Ref. 9 to provide a confirmation of Allen's theory,[3] based on a 1-**k** magnetic structure. On the contrary, the interpretation of the spin-wave dispersion in UO_2 on the basis of a 3-**k** structure[10] could not account for most of them. If the magnetic structure is 3-**k**,

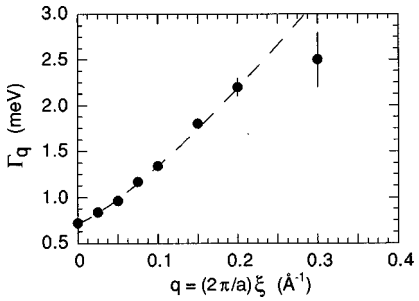

FIG. 11. Plot of the full width at half maximum of the low-energy magnetic response at $T=31.7$ K versus the amplitude of the wave vector $q=(2\pi/a)\xi$. The solid line is a fit to the function $\Gamma=\Gamma_0+\alpha q^\gamma$ (see text).

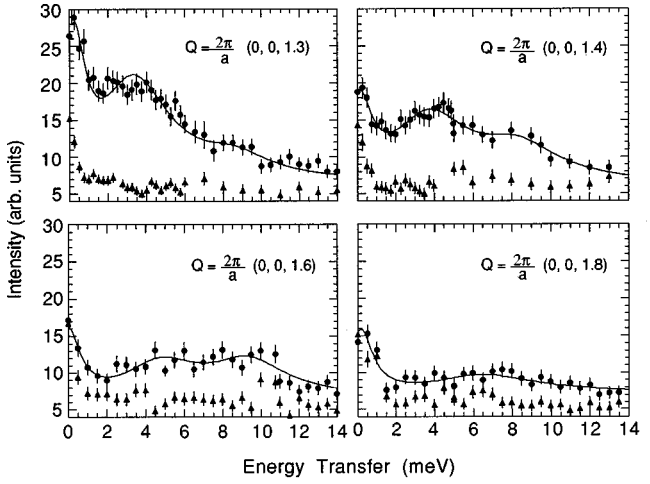

FIG. 12. Magnetic excitation spectra at $T=65.5$ K and different $\mathbf{Q}=(2\pi/a)(0,0,2-\xi)$. Solid lines are the fit to a flat background and the superposition of two Lorentzian line shapes. Closed circles represent intensity measured in the spin-flip channel, triangles correspond to non-spin-flip data.

the crystal is single domain and the magnetic modes (without magnon-phonon interaction) along the Γ-X direction should belong to two ''spin'' branches which are degenerate at Γ. Following Ref. 10, two ''quadrupolar'' branches should also be present, which, however, correspond to modes of intensity much smaller than that of the spin modes (typically by a factor 10^{-2}).

The dispersion curves for the spin modes in a 3-$\mathbf{k}$ magnetic structure were calculated for USb in Refs. 20 and 21. We have applied to UO_2 the method outlined in Ref. 21, using the CF wave functions given in Ref. 14. Following this approach, which involves the two ''spin'' modes only, it is possible to fit the dispersion of the strong excitations observed in the neutron-scattering spectra; however, a good fit of the experimental data can only be obtained if the exchange interaction is assumed to be anisotropic, with a sign of the anisotropy which would favor a longitudinal rather than the transverse magnetic structure revealed by neutron diffraction. Furthermore, the exchange parameters which are needed to fit the experimental observations are too large and would correspond to a transition temperature $T_N \sim 45$ K (the same inconsistency was obtained in Ref. 10). Reducing the magnitude of the exchange parameters to improve the calculated value of T_N leads to an even larger anisotropy, always in the wrong direction.

Moreover, in this simple approximation, the presence of the weaker excitations shown in Fig. 2 cannot be explained. For example, along the Γ-X direction, the ''optical'' spin branch and the ''acoustic'' one must be degenerate at the Γ point, and the optical branch must have the same energy, of ~ 10 meV, at the Γ and X points. Thus the modes at ~ 12 meV (those corresponding to the open diamonds in Fig. 2) cannot lie on this branch. A possible explanation is that they belong to a quadrupolar branch, as assumed in Ref. 10. Their intensity could be enhanced by the spin-lattice interaction, so much as to become comparable to that of the dipolar peaks in the central region of the Γ-X line (see Fig. 1).

In conclusion, to reproduce the spin-wave dispersion determined in Ref. 4, and confirmed by the present polarized-neutron experiment, it is necessary to include in the theoretical model the quadrupolar effects and the interaction with the lattice.

B. $T > T_N$

The most significant result in the paramagnetic region is the dispersive inelastic response observed between 3 and 10 meV. Although weak, this signal was easily measurable even at 200 K, more than six times the Néel temperature. Before continuing to discuss possible explanations for this inelastic spectrum in the *paramagnetic* state it is worth stressing two points. First, the crystal-field peaks in UO_2 have been measured[14] and the first excited level above the Γ_5 triplet ground state is at 150 meV, so that these inelastic features are *not* associated with transitions between different levels of the paramagnetic CF states. They must arise from within the Γ_5 ground state. The question then is: what mechanism splits the triplet ground state and how? Second, the *spatial* correlations between the uranium spins are very weak above 40 K. This has already been reported in earlier work[9] and may be seen by noting that Fig. 10 shows a spatial correlation of only ~ 5 Å (i.e., nearest neighbors) at 31.7 K, just above T_N. This point can be gathered directly from Fig. 12 by noting the magnitude of the signal at $E=0$, which represents the signal coming from the *spatial* correlations of the paramagnetic U moments. For example, the signal falls by a factor 2 only on changing ξ from 1.3 to 1.6 (left-hand panels). If this signal were uniform across the Brillouin zone it would indicate *no* spatial correlations at all. In fact, they are weak, and disappear completely by ~ 100 K, but the inelastic features remain.

The weakness of spatial correlations in the paramagnetic phase, and the lack of an inelastic-to-quasielastic crossover at a temperature-dependent wave vector (as qualitatively observed, e.g., in Gd),[22] preclude an interpretation of the inelastic features in terms of paramagnetic spin waves.

For the same reason, it can be excluded that the inelastic response observed above T_N is a consequence of short-range quadrupolar order, with associated distorted clusters coherently fluctuating. In fact, the quadrupolar correlation length in the paramagnetic phase should diverge at a lower temperature than the magnetic correlation length, if the first-order transition did not interrupt their growth.[3] Therefore it seems reasonable to assume that the quadrupolar correlation length between 40 and 200 K is even shorter than the magnetic one (or, at least, not much longer). Spin and/or quadrupole dynamical correlations due to ion-ion couplings not associated with short-range order could, in principle, be present.[23,24] These correlations, which would persist up to infinite temperature, are usually interpreted in terms of a random molecular field acting on the ions at high T. However, the features we measure, and in particular their clear inelastic character, do not correspond to what is expected for this type of correlations.

Below T_N, the mean-field–random-phase approximation (MF-RPA) analysis performed in Refs. 3 and 10 yields an AF state associated to a distortion of the oxygen cage, quadrupolar order being induced as a secondary order parameter

by the primary magnetic order parameter. However, above T_N, both the molecular field and the lattice distortion vanish, and only unsplit CF levels would be expected. Apart from the application of the MF-RPA method, a major approximation made in Refs. 3 and 10 is the use of an effective quadrupolar interaction among the uranium ions; the electronic and phononic degrees of freedom are separated by implicitly assuming that the wave functions are direct products of CF and phonon functions while, in general, mixed ''vibronic'' states may exist. Within the so-called ''virtual-phonon'' technique, the mixed terms correspond to perturbative corrections to the wave functions. Whenever these corrections are appreciable, a dynamical Jahn-Teller effect (DJTE) can be anticipated. By the above discussion, we have tried to demonstrate that the observed signal cannot be satisfactorily explained by corrections to the MF-RPA method applied to the effective-interaction model. An explanation must therefore be sought in the neglect of DJTE-type mixing, which is implicit in the use of this model.

A well established theoretical framework for the DJTE exists only in the simplest cases, in which a single ion interacts with one or a few phonon modes.[25] For the much more complex case relevant to UO_2, i.e., a lattice of DJTE ions with shared ligands interacting with the whole phonon continuum, and interacting between themselves through magnetic superexchange, the theoretical problem is extremely difficult, and the situation is not clear at all. In the following, an interpretation of the data in terms of a semiphenomenological model will be given.

It is known that below 200–300 K a single-ion DJTE reduces the effective g factor of the static susceptibility of UO_2 diluted in ThO_2 (Ref. 5) (this is an example of the so-called ''Ham effect''). It is tempting to consider that the observed inelastic signal may be the dynamical counterpart of this static effect. The DJTE in the solid solution is due to the coupling of the Γ_5 CF ground state of the uranium ions with tetragonal (Γ_3) and trigonal (Γ_5) distortions of the oxygen cage, i.e., the same coupling giving birth to effective ion-ion quadrupolar interactions in nondiluted UO_2.

In the single-ion case, the oxygen cage may be qualitatively thought as oscillating between equivalent tetragonal or trigonal distortions, with a characteristic frequency which can range from zero (static or strong-coupling Jahn-Teller effect) to typical phonon frequencies (weak-coupling Jahn-Teller effect). In the strong single-ion DJTE limit, a decoupling of CF and phonon states occurs, just as when the Jahn-Teller coupling is zero, but the CF states correspond to a distorted environment, and we may expect for them a finite width proportional to the characteristic fluctuation frequency. In UO_2, this is typically $\leqslant 10^{12}$ Hz, i.e., substantially less than the Debye frequency $\nu_D \approx 5\times 10^{12}$ Hz. Thus, we interpret the inelastic signal below 10 meV as reflecting features associated with the static limit.

Both tetragonal and trigonal quasistatic distortions would split the ground-state triplet into a doublet and a singlet. Therefore distortions of this kind cannot explain the experimental data, as we observe at least two broad peaks with distinct energies (anisotropic exchange could split the dispersion branch but, as discussed below, this is a minor effect). Instead, the observed signal agrees surprisingly well with what is expected for a monoclinic distortion of the oxygen cage of the same type (1-**k**), and of about the same size, as that assumed to occur below T_N in Ref. 6. This distortion consists in an alternate shift of the oxygen planes perpendicular to a cubic axis and will occur with equal probability for each of the three equivalent crystallographic directions. Thus we are led to the conclusion that in the paramagnetic phase of UO_2, which can be considered as a lattice of DJTE centers, the coherent motion of neighboring oxygen cages produces 1-**k** distortions rather than the tetragonal or trigonal single-ion distortions which occur below T_N in the 3-**k** ordered phase.

The peaks we observe in our experiment display dispersion, with the smallest energy at the magnetic zone center. The dispersion may be attributed to superexchange interaction between uranium ions in distorted clusters, introducing a wave-vector dependence of the single-ion excitation energy (the so-called ''magnetic exciton'').[26,27] Since the retardation of superexchange interactions should be negligible with respect to the fluctuation time of the clusters, we have simply tried to fit our measurement to a standard RPA model of the dynamics, including a monoclinic distortion.

The Hamiltonian of the system is given by

$$H = H_{\mathrm{CF}} + H_{\mathrm{int}}, \tag{3}$$

where

$$H_{\mathrm{CF}} = \sum_{n,m} B_n^m \hat{O}_n^m, \tag{4}$$

and

$$H_{\mathrm{int}} = -\sum_{i<j} \mathcal{J}_{ij} \mathbf{J}_i \cdot \mathbf{J}_j. \tag{5}$$

The CF on uranium ions in UO_2 under monoclinic distortions is described in detail in Ref. 14, where H_{CF} is explicitly written in terms of the intervening operator equivalents $\hat{O}_n^m$ in Eqs. (8)–(10). The CF wave functions and the eigenvalues are also given by formulas (11)–(15).

We assume for simplicity that the exchange is isotropic. It must be noted that exchange anisotropy would produce a doubling of the dispersion branch of the magnetic exciton. However, even a ratio of the order of 0.6 between the two components $\mathcal{J}_\parallel$ and $\mathcal{J}_\perp$ of the exchange tensor, as assumed in Ref. 10, could not explain a separation of more than 4 meV between the two peaks at (0,0,1.4) and (0,0,1.6) in Fig. 12. A more isotropic exchange is also favored by spin-phonon interaction.[9] For this reason we attributed the two peaks to two distinct CF transitions and we neglected the effect of exchange anisotropy in performing this analysis.

The excitations of the system in the RPA are given by the poles of the dynamical susceptibility,

$$\chi(\mathbf{q},\omega) = \frac{\chi_0(\omega)}{1 - \mathcal{J}(\mathbf{q})\chi_0(\omega)}, \tag{6}$$

where $\mathcal{J}(\mathbf{q})$ is the Fourier transform of $\mathcal{J}_{ij}$.[10] The function $\chi_0(\omega)$ is the single-ion, frequency dependent susceptibility for a system of noninteracting ions in the CF, which is given by Ref. 26:

$$\chi_0(\omega)=\sum_{n,m}^{E_n\neq E_m}|M_{nm}|^2\frac{\Delta_{nm}}{\Delta_{nm}^2-(\omega+i\epsilon)^2}(p_m-p_n)+\frac{\delta_{\omega,0}}{T}\sum_{n,m}^{E_n=E_m}|M_{nm}|^2p_n. \quad (7)$$

The sum in Eq. (7) runs over the CF states in the ground manifold. Their splittings and populations (at the temperature T) are $\Delta_{nm}=E_n-E_m$ and $p_n=\exp(-E_n/T)/Z$, respectively, Z being the partition function. M_{nm} is the dipolar matrix element between the states n and m.

The dispersion curves have been calculated starting from the CF parameters in Table IV of Ref. 14, corresponding to the nearest neighbors, intermediate coupling (IC) model for a lattice distortion of 0.014 Å. This leads to three singlets ($|\psi_i\rangle$, $i=1,2,3$) with energy separations $\Delta_{21}=3.9$ meV and $\Delta_{31}=8.4$ meV, and matrix elements $|M_{12}|^2=6.96$, $|M_{13}|^2=6.25$, and $|M_{23}|^2=5.56$. In the isotropic case, along the Γ-X direction, we have

$$\mathcal{J}(q)=4\mathcal{J}_0\left(1+2\cos\frac{aq}{2}\right), \quad (8)$$

so that $\mathcal{J}(q_{AF})=-4\mathcal{J}_0$ for $q_{AF}=(2\pi/a)$, $\mathcal{J}_0$ being negative for antiferromagnetic coupling. At the other extreme, $q_F=0$, we have $\mathcal{J}(q_F)=12\mathcal{J}_0$.

The value of $\mathcal{J}(q_{AF})$ has been obtained by assuming that the lowest energy mode becomes soft at T_N for $q=q_{AF}$. This assumption must be taken with caution, since the ordered phase has been found to be 3-**k**. However, the value we calculate, $\mathcal{J}(q_{AF})=0.44$ meV, is consistent both with the values 0.48 and 0.40 meV used in Ref. 14 to obtain the self-consistent solution for the ordered moment in the 1-**k** and in the 3-**k** models, respectively. Moreover, it is of the same order as $\mathcal{J}(q_{AF})\simeq 0.54$ meV, obtained in Ref. 9 from the analysis of the critical scattering anisotropy (after multiplying by a factor 2 and changing the sign to fit our notation).

The dispersion curves calculated at 65.5 K are shown in Fig. 13, where the experimental points deduced from the neutron spectra in Fig. 12 are also reported. The dashed line corresponds to the transition from $|\psi_2\rangle$ to $|\psi_3\rangle$, which is less intense, since the first excited singlet becomes populated only by increasing the temperature. The relative intensity of the transitions have also been calculated. The sum of the intensities of the two lowest (not resolved) branches is higher than that of the highest branch by a factor 1.2 at q_{AF}, which decreases to 1.1 at q_F. The intensities of the two peaks is reduced by about a factor 2 by increasing $(a/2\pi)Q$ from 1 to 2, in line with the experimental observations.

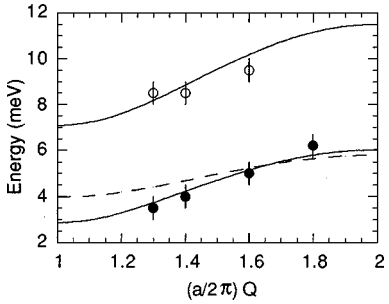

FIG. 13. Dispersion curves along the $(0,0,2-\xi)$ direction of the magnetic excitons in the paramagnetic phase. The dashed line corresponds to the weak transition between the two excited singlets, which is not resolved in our experiment.

V. CONCLUSION

Inelastic neutron scattering with full polarization analysis has been used to study the magnetic response of uranium dioxide, both above and below the antiferromagnetic ordering temperature. The results obtained by Cowley and Dolling[4] in the AF phase have been confirmed; evidence of magnon-phonon interactions along the $(0,0,\xi)$ direction is given by the splitting of the lowest spin-wave branch, and by the wave-vector dependence of the energy-integrated dynamic susceptibility. The spin-wave dispersion is strongly modified by these interactions, and does not compare favorably with MF-RPA predictions, either assuming a 3-**k** or a 1-**k** type of magnetic order. However, the assumption of a 3-**k** magnetic structure allows a more simple description of the excitation modes than the multidomain 1-**k** hypothesis.

A dispersive inelastic response arising from within the Γ_5 ground state has been observed in the paramagnetic phase, well above the Néel temperature where the spatial spin-spin correlation is found to be negligible. We have shown that the experimental spectra can be interpreted assuming a dynamical JT distortion of the oxygen cage, with monoclinic (1-**k**) rather than trigonal (3-**k**) symmetry.

From the above results, a picture emerges in which local, uncorrelated 1-**k** dynamical JT distortions occur above T_N along the three directions of the $\langle 100\rangle$ star; as T_N is approached, a correlation builds up between the phases of the corresponding vibrations until, eventually, a static 3-**k** distortion condenses at T_N.

Further efforts should be made to confirm this idea. In particular, the impressive improvement of intensity and resolution obtained for direct-geometry chopper spectrometers at spallation neutron sources could justify new high-energy inelastic neutron-scattering experiments to examine the transitions from the ground triplet to the excited CF multiplets above T_N.

[1] B.C. Frazer, G. Shirane, D.E. Cox, and C.E. Olsen, Phys. Rev. **140**, A1448 (1965); B.T.M. Willis and R.I. Taylor, Phys. Lett. **17**, 188 (1965).
[2] O.G. Brandt and C.T. Walker, Phys. Rev. **170**, 528 (1968).
[3] S.J. Allen, Phys. Rev. **166**, 530 (1968); **167**, 492 (1968).
[4] R.A. Cowley and G. Dolling, Phys. Rev. **167**, 464 (1968).
[5] K. Sasaki and Y. Obata, J. Phys. Soc. Jpn. **28**, 1157 (1970).
[6] J. Faber and G.H. Lander, Phys. Rev. B **14**, 1151 (1976), and references therein.
[7] J. Rossat-Mignod, in *Methods of Experimental Physics*, edited by K. Sköld and D.L. Price (Academic Press, New York, 1987), Vol. 23C, pp. 69–158.

[8] P. Burlet, J. Rossat-Mignod, S. Quezel, O. Vogt, J.C. Spirlet, and J. Rebizant, J. Less-Common Met. **121**, 121 (1986).
[9] W.J.L. Buyers and T.M. Holden, in *Handbook of the Physics and Chemistry of the Actinides*, edited by A.J. Freeman and G.H. Lander (North-Holland, Amsterdam, 1985), Vol. 2, p. 239.
[10] P. Giannozzi and P. Erdös, J. Magn. Magn. Mater. **67**, 75 (1987).
[11] E. Holland-Moritz and G.H. Lander, in *Handbook of the Physics and Chemistry of Rare Earths*, edited by K.A. Gschneidner, L. Eyring, G.H. Lander, and G. Choppin (Elsevier Science, Amsterdam, 1994), Vol. 19, pp. 1–121.
[12] H.U. Rahman and W.A. Runciman, J. Phys. Chem. Solids **27**, 1833 (1966).
[13] S. Kern, C.-K. Loong, and G.H. Lander, Phys. Rev. B **32**, 3051 (1985).
[14] G. Amoretti, A. Blaise, R. Caciuffo, J.M. Fournier, M.T. Hutchings, R. Osborn, and A.D. Taylor, Phys. Rev. B **40**, 1856 (1989).
[15] K.A. McEwen, U. Steigenberger, and J.L. Martinez, Physica B **186-188**, 670 (1993); **213-214**, 128 (1995); M.B. Walker, C. Kappler, K.A. McEwen, U. Steingenberger, and K.N. Clausen, J. Phys.: Condens. Matter **6**, 7365 (1994).
[16] P. Santini and G. Amoretti, Phys. Rev. Lett. **73**, 1027 (1994); P. Santini, Phys. Rev. B **57**, 5191 (1998).
[17] L. Paolasini, R. Caciuffo, B. Roessli, and G.H. Lander, Physica B **241-243**, 681 (1998); Phys. Rev. B **59**, 6867 (1999).
[18] R.M. Moon, T. Riste, and W.C. Koehler, Phys. Rev. **181**, 920 (1969).
[19] E. Riedel and F. Wegner, Phys. Rev. Lett. **24**, 730 (1970).
[20] J. Jensen and P. Bak, Phys. Rev. B **23**, 6180 (1981).
[21] B. Hälg, and A. Furrer, Phys. Rev. B **34**, 6258 (1986).
[22] J.W. Cable and R.M. Nicklow, Phys. Rev. B **39**, 11 732 (1989).
[23] M. Blume and J. Hubbard, Phys. Rev. B **1**, 3815 (1970).
[24] M. Takahashi, J. Phys. Soc. Jpn. **52**, 3592 (1983).
[25] I.B. Bersuker and V.Z. Polinger, *Vibronic Interactions in Molecules and Crystals* (Springer-Verlag, Berlin, 1989).
[26] P. Fulde, in *Handbook on the Physics and Chemistry of Rare Earths*, edited by K.A. Gschneider, Jr. and L. Eyring (North-Holland, Amsterdam, 1979), Vol. 2, p. 295.
[27] J. Jensen and A.R. Mackintosh, *Rare Earth Magnetism, Structures and Excitations* (Clarendon Press, Oxford, 1991).